Rodlike particles in gas discharge plasmas: Theoretical model

A. V. Ivlev,[1] A. G. Khrapak,[2] S. A. Khrapak,[1] B. M. Annaratone,[1] G. Morfill,[1] and K. Yoshino[3]
[1]*Centre for Interdisciplinary Plasma Science, Max-Planck-Institut für Extraterrestrische Physik, D-85741 Garching, Germany*
[2]*Institute for High Energy Densities RAS, 125412 Moscow, Russia*
[3]*Department of Electronic Engineering, Osaka University, 565-0871 Osaka, Japan*
(Received 10 March 2003; published 12 August 2003)

Recently, complex plasmas with strongly asymmetric (rodlike) particles were investigated experimentally in rf and dc discharges [V. I. Molotkov *et al.*, JETP Lett. **71**, 102 (2000); B. M. Annaratone *et al.*, Phys. Rev. E **63**, 036406 (2001)]. In this paper, a theoretical model is proposed which describes the behavior of such systems. Major results of the proposed model are the following: Equilibrium charge is calculated for particles orientated perpendicular and parallel to the ion flux (electric field); equilibrium states of particles (orientation angle and levitation height) are obtained; energy of electrostatic interaction between rods is derived, depending on the mutual orientation. Comparison of experimental and theoretical results shows quite good agreement. In conclusion, some important theoretical issues as well as possible new experiments are discussed.

DOI: 10.1103/PhysRevE.68.026403 PACS number(s): 52.27.Lw, 61.30.Gd, 83.80.Hj

I. INTRODUCTION

Crystallization of charged microparticles in a radio-frequency (rf) [1–3] and dc [4–6] discharges was discovered about one decade ago. This triggered enormous interest to study properties of strongly coupled complex (dusty) plasmas. Currently, experimental and theoretical investigations in this field are going on in many laboratories throughout the world. Recent reviews [7–9] discuss various aspects of the complex plasma crystallization.

So far, almost all complex plasma experiments were performed with particles of a spherical form. Also, theoretical investigations usually neglect the grain shape, assuming spherical particles. It is well known, however, that colloidal suspensions, which have many common properties with complex plasmas, exhibit variety of possible states in the case of strongly asymmetric particles [10,11]. Along with a liquid phase, several liquid-crystalline and crystalline phases have been observed. Difference between these phases is determined by the positional and orientational ordering. Just recently, levitation and formation of ordered structures in the subsystem of very long rodlike particles—*needles* or *rods* (length-to-radius or aspect ratio varied from 80 up to 240)—suspended in dc striations and rf sheaths have been reported [12,13]. Also, levitation of weakly asymmetric grown particles (aspect ratio ~ 3) in a rf plasma has been observed [14].

The rf discharge experiments with rods [13] were performed in a Gaseous Electronics Conference (GEC) reference cell [15] filled with krypton or argon gas. The nylon (density $\simeq 1.1$ g/cm^3) particles of diameters 7.5 μm and lengths of 300 μm and 600 μm were used. Among those ''monodisperse'' particles, there was a small fraction of very long ''freak'' particles of 1–3 mm length. Levitation of needles was observed in a rf sheath, where electrostatic force on charged particles balances the gravity. The particles formed a horizontal disk-shaped layer. Longer rods floated horizontally, mainly in the center of the system, while the shorter rods settled around vertically—parallel to the strong electric field of the sheath, as shown in Fig. 1. The horizontal rods floated near the top of the vertical ensemble in the central region, and near the bottom at the periphery. Usually, the vertical rods arranged themselves in ordered hexagonal structures, similar to those observed in experiments with spherical particles. Levitation of the rods was only possible for the discharge pressure above 5 Pa and power higher than about 20 W.

For experiments in a dc plasma [12], the same particles were used. The experiments were performed in the discharge tube [5] filled with neon gas. The rods were suspended in strong electric field existing inside standing striations. Particles formed ordered hexagonal structures in horizontal layers, with a few layers evenly spaced in the vertical direction. All the rods, irrespective of the size, were oriented horizontally, being aligned in the same direction, as shown in Fig. 2. Similar to the rf experiments, relatively high discharge power was necessary to levitate the particles. Generally, it was more difficult to suspend larger particles. In order to levitate them, a neon-hydrogen mixture was used, which caused steepening of the electric field profile inside the striations.

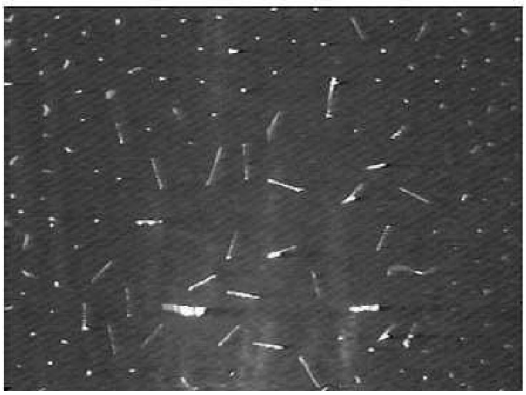

FIG. 1. Top view on rodlike particles levitating in a rf sheath (from Ref. [13]). Dots at the periphery are vertically oriented ''short'' rods ($L=300$ μm); ''long'' particles ($L \geqslant 600$ μm) levitate horizontally in the center.

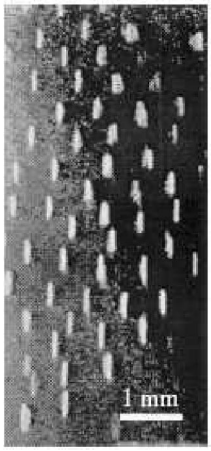

FIG. 2. Top view on rodlike particles levitating in a dc striation (from Ref. [12]). Irrespective of the particle length, the levitation is always horizontal.

In this paper, we make an attempt to formulate a consistent quantitative approach for description of complex processes which determine the behavior of rodlike particles immersed in a plasma with a strong electric field. We analyze relevant physical mechanisms and major plasma processes involved, and compare theoretical results with experimental observations. The paper is organized as follows: In Sec. II, the electric potential distribution around very elongated rods is defined. In Sec. III, the equilibrium charge on a rod is calculated for particles orientated perpendicular and parallel to the ion flux (electric field). In Secs. IV and V the equilibrium states of a rod (orientation angle and levitation height) suspended in external electric field are derived. In Sec. VI, the influence of the ion drag force on the equilibrium states is discussed. In Sec. VII, the energy of electrostatic interaction between rods is calculated, depending on the mutual particle orientation. Finally, in Sec. VIII, we compare major experimental and theoretical results and show that there is quite good agreement between them. We also discuss some important theoretical issues that need to be analyzed in future, as well as possible experiments that would allow us to check the proposed theory more carefully.

II. POTENTIAL OF A UNIFORMLY CHARGED ROD

First, we consider the case of *uniformly charged* dielectric cylinder (rod) with the total charge $Q<0$, length L, and radius a. Simple integration yields the following expression for the electrostatic potential around the rod (in the absence of the plasma screening):

$$\phi_r(\rho,z)=\lambda_0[\ln(\xi_+ + \sqrt{\xi_+^2+1})+\ln(\xi_- + \sqrt{\xi_-^2+1})], \tag{1}$$

$$\xi_\pm=(\tfrac{1}{2}L\pm z)/\rho,$$

where $\lambda_0=Q/L$ is the linear charge density, (ρ,z) are the cylindrical coordinates with the origin in the center of the rod, z is pointed along the rod axis. In the vicinity of the middle part of the rod, $|z|\ll L$ and $a\leqslant\rho\ll L$, the potential changes as $\phi_r\simeq 2\lambda_0\ln(L/\rho)-4\lambda_0(z/L)^2$, i.e., the radial potential distribution coincides with that for an infinite charged string. Far from the particle, when $\sqrt{\rho^2+z^2}\equiv r\gg L$, the first term in the expansion of Eq. (1) corresponds to the isotropic potential of a pointlike charge, $\phi_r\simeq Q/r$. The screening becomes important at $r\gtrsim\lambda_{De}$, where λ_{De} is the (electron) Debye length. (Both in rf sheaths and dc striations, the ion drift velocity exceeds significantly the thermal velocity, and, hence, ions do not contribute to the screening.) In experiments, λ_{De} usually exceeds the particle length, and therefore we can use the ''vacuum limit'' potential (1) for the estimations below.

For conductive particles the self-consistent charge distribution is not uniform, but changes along the rod in order to provide *constant surface potential*. For the cylindrical conductive particle the problem cannot be solved analytically, but we can consider the rod as an axially symmetric ellipsoid, with the semiaxes $L/2$ and a. The resulting expression for the potential around the ellipsoid [16] is more complicated than Eq. (1), but in fact these expressions converge as the ratio L/a increases. If the parameter Λ which characterizes elongation of the particle,

$$\Lambda=\ln(L/a),$$

is sufficiently large (for experiments, $L/a=80$–240, so that $\Lambda\simeq 4.4$–5.5), then Eq. (1) and the potential of the conductive ellipsoidal particle coincide with accuracy $o(\Lambda^{-1})$: The self-consistent surface charge density for the ellipsoid is almost constant in the middle [16], and deviates noticeably from the uniform distribution only in narrow regions close to the ends: $L/2-|z|\lesssim L/\Lambda$. Capacity of the rod tends to the capacity of the conductive ellipsoid, $C_r\simeq Q/\phi_r(a,0)\simeq L/2\Lambda$ [16].

III. CHARGING OF A ROD

Let us study charging of a *conductive* rod immersed in a homogeneous ion flow. Practically, a rod can be called ''conductive'' when the charge (electron) redistribution due to conductivity is much faster than the plasma processes determining the charging. The time scale of the conductive charge relaxation is of the order of the electron resistivity of the particle material [17]. For any conductor material, this is much shorter than the charging time scale due to the plasma absorbtion [18]. Therefore, electrons in the particle redistribute themselves in such a way that the resulting surface potential is kept constant. Hence, instead of calculating the ion flux density at each element of the particle surface, it is sufficient to solve much simpler problem—to determine the total ion flux on the particle.

In order to obtain the ion absorption (collection) cross section. one has to calculate the deflection of the ion trajectories due to the electric field of the rod. We neglect the influence of the external (rf sheath or dc striation) electric field which (i) polarizes the rod and (ii) changes trajectories of ions while they interact with the rod field. As discussed in the preceding section, for $\Lambda\gg 1$ the constant surface potential actually implies the constant charge density. Thus, we assume the uniform surface charge distribution and use the potential given by Eq. (1). (In the following section, we dis-

cuss how the charge distribution is changed due to the polarization.) Influence of the external field on the ion trajectories can be neglected when the external potential does not change strongly along the rod, i.e., when its spatial scale is larger than L. We suppose that this condition is satisfied. In addition, the ion motion is supposed to be collisionless—the ion mean free path should exceed L.

Experiments [12,13] show that only two types of the rod orientation are possible—perpendicular (horizontal) or parallel (vertical) to the external electric field. Below we consider these cases.

A. Horizontal rods

The rod axis is perpendicular to the flux of ions. The ion drift velocity, u, exceeds significantly the thermal velocity, $v_{T_i}=\sqrt{T_i/m_i}$ (it is typical both for rf sheaths and dc striations, where particles usually levitate). Equilibrium charge is determined by the balance of the ion and electron fluxes on the rod surface, $J_e-J_i=0$. The flux for the Boltzmann distributed electrons is $J_e=\sqrt{2\pi}aLn_e v_{T_e}e^{-\gamma_r}$ [19], where $\gamma_r=2\Lambda e|Q|/LT_e\equiv(|Q|/C_r)/(T_e/e)$ is the dimensionless particle potential (in units T_e/e), and $v_{T_e}=\sqrt{T_e/m_e}$ is the electron thermal velocity. The ion flux is $J_i=2\rho_h Ln_i u$, where the absorption impact parameter (radius) for the horizontal cylinder, $\rho_h=a\sqrt{1+2\gamma_r/M^2}$, is given by the orbital motion limited (OML) expression [20], $M=u/c_s$ is the Mach number, and $c_s=\sqrt{T_e/m_i}$ is the ion acoustic velocity. We note again that the particles are assumed to be sufficiently elongated, $\Lambda\gg 1$ (condition $\rho_h\ll L$ should also be satisfied). Then we can neglect the ''end effects'' [21] and obtain the following equation for the particle potential (charge) γ_r:

$$\sqrt{\frac{\pi}{2}\frac{m_i}{m_e}}\frac{n_e}{n_i}=\sqrt{M^2+2\gamma_r}e^{\gamma_r}. \tag{2}$$

The dependence γ_r versus M for the horizontal rod calculated from Eq. (2) ($n_e/n_i=1$, argon gas) is plotted in Fig. 3 (solid line). At small M, the charge asymptotically tends to the value corresponding to an infinite cylinder in an isotropic (bulk) plasma [19]. Note that this value does not depend on the ion temperature as long as the Debye screening can be neglected (the OML approach is valid) and if $T_i/T_e\ll\gamma_r$.

B. Vertical rods

In the beginning, we neglect the thermal motion of ions and assume $T_i=0$. The rod axis z is pointed upward, and ions drift down with velocity $-u$. Then the radial motion towards the rod in field (1) is given by the following equation:

$$\ddot{\tilde{\rho}}=-\frac{1}{2}\left(\frac{1-\tau}{\sqrt{(1-\tau)^2+\tilde{\rho}^2}}+\frac{\tau}{\sqrt{\tau^2+\tilde{\rho}^2}}\right)\frac{\mathcal{E}_Q}{\mathcal{E}_u}\frac{1}{\tilde{\rho}}. \tag{3}$$

To make formulas shorter we introduced the potential energy scale $\mathcal{E}_Q=e|Q|/L$ and the initial kinetic energy $\mathcal{E}_u=\frac{1}{2}m_i u^2$, as well as the dimensionless radial coordinate $\tilde{\rho}=\rho/L$ and time $\tau=ut/L$ (dots denote derivatives with respect to τ). The particle field does not affect considerably the ion motion along the z axis: Ratio of the energy that ions can gain in the field, $\lesssim\Lambda\mathcal{E}_Q$, to the kinetic energy $\mathcal{E}_u$ is $\lesssim M^{-2}\Lambda(\mathcal{E}_Q/T_e)$. The ion flux is supersonic, and the self-consistent calculations of the charge (see the end of this section) show that the factor $\Lambda(\mathcal{E}_Q/T_e)\equiv\gamma_r/2$ is about unity. Therefore, the vertical ion velocity can be approximately considered as constant. Then one can set the dimensionless time varying in the range $0\leqslant\tau\leqslant 1$ while an ion passes the rod (z changes from $L/2$ to $-L/2$).

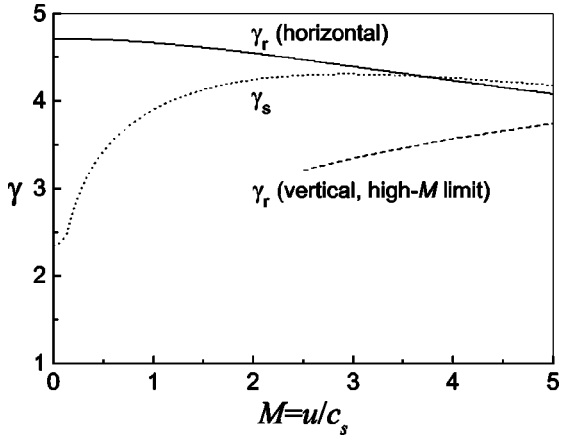

FIG. 3. Dimensionless potential of a rod of length L and radius a, $\gamma_r=2\Lambda e|Q|/LT_e$, versus the ion Mach number, $M=u/c_s$. Solid line corresponds to the horizontal rod [solution of Eq. (2)], dashed line shows the high-M limit for the vertical rod [solution of Eq. (6), valid for $M\gtrsim 3$]. Calculations are for argon gas and $\Lambda=\ln(L/a)=4.5$. For reference, dotted line shows the dimensionless potential of a spherical particle, $\gamma_s=e|Q|/aT_e$, calculated for $T_e/T_i=100$.

The motion of ions that are absorbed by the particle can be conditionally divided into two stages: At the first stage, ions approach the particle from ''infinity'' to $z\sim L/2$. At the second stage, they are deflected towards the rod and get absorbed at certain $z\gtrsim -L/2$. Far from the rod ($z\gg L/2$), Eq. (1) reduces to the Coulomb potential and the resulting force in the ρ direction ($\propto\rho/z^3$) is much weaker than the radial force when the ion passes the rod ($\propto\rho^{-1}$, at $-L/2\lesssim z\lesssim L/2$). Therefore, the relative variation of the radial coordinate (with respect to its initial value) is small at the first stage, $\sim\mathcal{E}_Q/\mathcal{E}_u\ll 1$ [22]. Also, the ratio of the radial velocities that ions acquire at the first stage, $\sim(\mathcal{E}_Q/m_i u)\tilde{\rho}$, and at the second stage, $\sim\sqrt{\Lambda\mathcal{E}_Q/m_i}$, is $\sim M^{-1}\sqrt{\Lambda^{-1}(\mathcal{E}_Q/T_e)}\tilde{\rho}$. It is shown below that $\tilde{\rho}\lesssim 1$ (absorption radius is always less than the rod length), and thus the radial acceleration at the first stage is usually not important. Hence, we can assume that the ions start at $z=L/2$ ($\tau=0$) with the vertical (initial) velocity $-u$. The absorption radius for the vertical rod, $\tilde{\rho}_v\equiv\tilde{\rho}(0)$, is determined by the solution of Eq. (3) with the initial condition $\dot{\tilde{\rho}}(0)=0$ and the absorption condition $\tilde{\rho}(1)=0$ (for simplicity, $\tilde{\rho}$ at $\tau=1$ is set equal to zero instead of $a/L\sim 10^{-2}$). Integrating Eq. (3) numerically with these con-

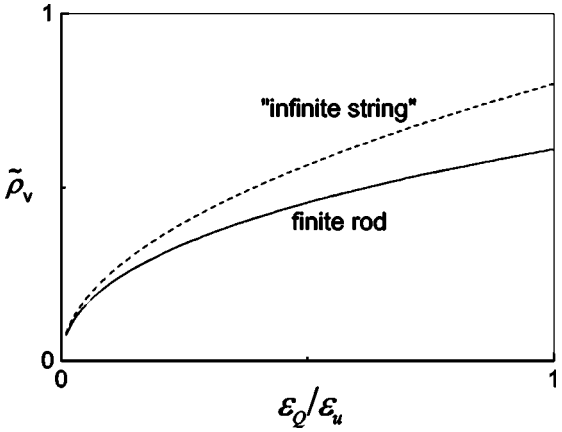

FIG. 4. Dimensionless ion absorption radius for the vertical rod of the length L, $\tilde{\rho}_v=\rho_v/L$, versus the ratio of the Coulomb to ion kinetic energies, $\mathcal{E}_Q=e|Q|/L$ and $\mathcal{E}_u=\frac{1}{2}m_iu^2$. Solid line shows the results obtained after numerical integration of Eq. (3), dashed line is the analytical approximation, Eq. (5).

ditions we obtain the dependence $\tilde{\rho}_v$ versus $\mathcal{E}_Q/\mathcal{E}_u \propto M^{-2}(|Q|/L)$ (Fig. 4, solid line), from which we can finally deduce the absorption cross section $\pi\tilde{\rho}_v^2L^2$ as a function of the particle charge and the ion Mach number.

Equation (3) is derived for the potential of a finite cylinder [Eq. (1)]. This allows us to take into account the end effects—deviation from the logarithmic potential of an infinite string. In order to check how this deviation influences the value of $\tilde{\rho}_v$, we study the equation of ion motion in the field of the infinite string,

$$\ddot{\tilde{\rho}} \simeq -\frac{\mathcal{E}_Q}{\mathcal{E}_u}\frac{1}{\tilde{\rho}}, \tag{4}$$

applying the same initial and absorption conditions. the first integral of Eq. (4) yields the energy conservation $\dot{\tilde{\rho}}^2 = 2(\mathcal{E}_Q/\mathcal{E}_u)\ln(\tilde{\rho}_v/\tilde{\rho})$, from which we finally derive the expression for the dimensionless absorption radius,

$$\tilde{\rho}_v = \sqrt{\frac{2}{\pi}\frac{\mathcal{E}_Q}{\mathcal{E}_u}}, \tag{5}$$

shown in Fig. 4 (dashed line). Since $\mathcal{E}_Q/\mathcal{E}_u \equiv 2M^{-2}(\mathcal{E}_Q/T_e) \ll 1$, the absorption radius is always smaller than L. We also see that the difference between Eq. (5) and numerical solution of Eq. (3) is rather small in this range, so that the analytical expression (5) can be used for the order-of-magnitude estimate.

For certain conditions, the thermal ion motion can change significantly the flux on a vertical rod. The role of a finite ion temperature is discussed in detail in the Appendix. We found that for relatively high velocities of the ion flux, when the ratio $T_i/\mathcal{E}_u$ is sufficiently low, the thermal motion does not affect noticeably the ion absorption. Thus, for large M the ion flux on the vertical rod, $J_i \simeq \pi\rho_v^2 n_i u$, is determined by the absorption radius ρ_v from Eq. (5). Note that J_i on the vertical rod scales as $\propto L^2$, in contrast to $J_i \propto aL$ on the horizontal rod (neglecting logarithmic dependence), i.e., the ion flux on sufficiently long vertical particle can be anomalously high (similar effect was observed in probe measurements; see, e.g., Refs. [21,23]). Substituting the ion flux into the flux balance, we get the following equation for the high-M limit of the particle potential (charge):

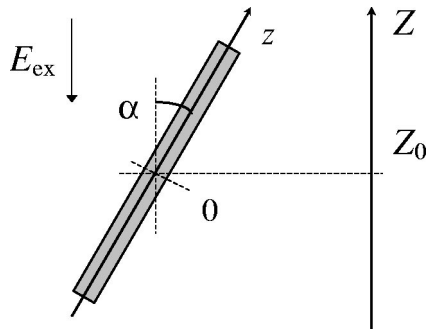

FIG. 5. Orientation of the rod with respect to the external electric field E_{ex}.

$$\sqrt{\frac{\pi}{2}\frac{m_i}{m_e}}\frac{n_e}{n_i}\frac{\Lambda}{e^{\Lambda}}M = \gamma_r e^{\gamma_r}. \tag{6}$$

The dependence of γ_r on M for the vertical rod calculated from Eq. (6) (for $\Lambda=4.5$) is plotted in Fig. 3 (dashed line). This high-M limit is valid for $M \gtrsim 3$. As follows from Eq. (6), the rod charge in the high-M limit depends also on Λ (almost linearly). However, this dependence is rather weak, especially for large M, and we can neglect it.

For smaller drift velocities the contribution of the thermal motion into the ion flux increases, and at low M the flux tends to the OML value for an isotropic (bulk) plasma. Correspondingly, the particle potential is represented by the low-M asymptote for a horizontal rod (solid line in Fig. 3). Hence, the dependence $\gamma_r(M)$ for the vertical rod lies in between the two curves—solid and dashed lines in Fig. 3—and approaches them asymptotically in the low- and high-M limits, respectively.

IV. CHARGE DISTRIBUTION ON A ROD IMMERSED IN ELECTRIC FIELD

In the presence of an external electric field, the induced nonuniform charge distribution on the surface of a conductive rod provides constant surface potential. Consider a rod immersed in a weakly inhomogeneous electric field, $E_{ex}(Z)$. The field is a function of the vertical coordinate (height) Z and is pointed in the direction opposite to Z. The rod axis is tilted by angle α with respect to the field direction, as shown in Fig. 5. The longitudinal rod coordinate z (with $z=0$ at the rod center) and the vertical coordinate are related by $Z=Z_0+z\cos\alpha$, with Z_0 the vertical coordinate (height) of the rod center and $-L/2<z<L/2$. Expanding the field around the rod center, $E_{ex}(Z_0,z)=E_0+E_0'z\cos\alpha+\cdots$, we get the electric potential of the external field along the rod,

$$\phi_{ex}(Z_0,z)=\phi_0-E_0 z\cos\alpha-\frac{1}{2}E_0' z^2\cos^2\alpha-\cdots,$$

with $E_0=-\phi_0', E_0'=-\phi_0'', \ldots$ functions of Z_0. The approximation of a ''weakly inhomogeneous field'' means that the spatial scale of the field variation is much longer than the rod, $|E_0/E_0'|\equiv\ell_E\gg L$. Together with the condition $\Lambda\gg 1$ this allows us to omit the terms $o(L/\ell_E)$ and $o(\Lambda^{-1})$, and use the following expression for the linear charge density along the rod [16]:

$$\lambda(z)\simeq\lambda_0+\frac{E_0 z}{2\Lambda}\cos\alpha. \tag{7}$$

We assume that the magnitude of the dipole part of the charge distribution [second term in Eq. (7)] is smaller than λ_0, i.e., $\frac{1}{2}(|E_0|L/\Lambda|\lambda_0|)\leqslant 1$—this allows us to use the Boltzmann distribution for the absorbed electrons. The inequality can be rewritten in a more convenient form: $e|E_0|L/\gamma_r T_e \leqslant 1$. For $L=300$ μm and $T_e\sim 1$ eV, this establishes the upper limit for the electric field, $|E_0|\lesssim 100$ V/cm. For spherical particles of 3–10 μm in diameter, the field necessary for levitation in the rf sheath or dc striation is approximately one order of magnitude weaker [5,24]. Hence, we conclude that this restriction should be satisfied in experiments [12,13] with rodlike particles.

V. LEVITATION OF RODS IN ELECTRIC FIELD

Now let us study levitation of a rod suspended in an external (rf sheath or dc striation) electric field. The equilibrium state of the rod, the levitation height Z_0 and the orientation angle α with respect to the vertical axis, can be found considering the total potential energy of the particle, which includes the gravity contribution, $m_r g Z_0$. First, we assume no dependence of the particle charge on Z_0 and α. Then the energy is determined by the well-known expansion [17,25]:

$$U_\Sigma=m_r g Z_0+Q\phi_0-\tfrac{1}{2}d_Z E_0-\tfrac{1}{6}D_{ZZ}E_0'+\cdots, \tag{8}$$

with $E_0<0$ and $E_0'>0$ (note that the expansion also requires the external field to be weakly inhomogeneous—spatial scale of its variation should be larger than the rod length). The dipole term in Eq. (8) is given by the Z projection of the dipole moment [16], $d_Z=d_\parallel\cos\alpha+d_\perp\sin\alpha$, which is due to polarization [Eq. (7)]. The longitudinal dipole moment of the rod, $d_\parallel\simeq\frac{1}{24}(E_0L^3/\Lambda)\cos\alpha$, is much larger than the transverse one, $d_\perp\sim d_\parallel(a/L)^2\tan\alpha$, so that we get $d_Z\simeq d\cos^2\alpha$, where

$$d=\frac{E_0L^3}{24\Lambda}<0 \tag{9}$$

is the magnitude of the dipole moment [16]. The quadrupole term in Eq. (8) is determined by the ZZ compound of the quadrupole tensor of the rod, D_{ij} [16,25]. The tensor transformation yields $D_{ZZ}=D_\parallel\cos^2\alpha+D_\perp\sin^2\alpha$, with $D_\parallel\simeq\frac{1}{6}QL^2$ and $D_\perp=-\frac{1}{2}D_\parallel$ the principal values of the tensor. From that we get $D_{ZZ}\simeq\frac{1}{2}D(3\cos^2\alpha-1)$, where

$$D=\frac{QL^2}{6}<0 \tag{10}$$

is the magnitude of the quadrupole moment [16]. Note that the polarization does not affect the quadrupole moment. Substituting these results in Eq. (8) and retaining the first three terms in the electrostatic energy expansion, we obtain

$$U_\Sigma(Z_0,\alpha)\simeq m_r g Z_0+Q\phi_0-\frac{E_0^2L^3}{48\Lambda}\cos^2\alpha-\frac{QE_0'L^2}{72}\times(3\cos^2\alpha-1). \tag{11}$$

The equilibrium states are determined by the extrema of Eq. (11). From $\partial U_\Sigma/\partial Z_0=0$, we get the following for the levitation height:

$$m_r g-QE_0-\frac{E_0E_0'L^3}{24\Lambda}\cos^2\alpha=0.$$

This equation shows that in addition to the gravity and charge forces, the dipole force contributes to the balance in vertical direction, $m_r g=QE_0+dE_0'\cos^2\alpha$. However, this force does not affect the balance noticeably: In accordance with the restriction $e|E_0|L/\gamma_r T_e\leqslant 1$ which we imposed for Eq. (7), the dipole-to-charge force ratio is $\frac{1}{12}(L/\ell_E)(e|E_0|L/\gamma_r T_e)\ll 1$. Thus, the levitation height is mostly determined by the balance of the gravity and the overall charge forces, such as for a spherical particle. Note that the derived equilibrium is always stable, since $\partial^2U_\Sigma/\partial Z_0^2\simeq -QE_0'>0$.

We see from Fig. 3 that the magnitude of the dimensionless potential (charge) of a rod, $\gamma_r=2\Lambda e|Q_r|/LT_e$, is close to that of a spherical particle, $\gamma_s=e|Q_s|/aT_e$. From that we get the relation between the rod and sphere charges, $2\Lambda(Q_r/L)\sim Q_s/a$. The rod mass scales as $m_r\propto a^2L$ and the sphere mass as $m_s\propto a^3$. Then we conclude that the electric field necessary to balance the particle weight, $E_0\propto m/Q$, should be $\sim\Lambda$ times stronger for a rod, than for a spherical particle of the same radius. Therefore, rods should levitate $\sim\Lambda\ell_E$ below the level where spherical particles of the same radius are suspended. Note also that the m/Q ratio for rods has a very weak (logarithmic) dependence on L, and thus rods of different length (but of the same radius) should levitate at approximately the same level.

The equilibrium orientation is given by the condition $\partial U_\Sigma/\partial\alpha=0$ (torque balance):

$$\left(\frac{E_0^2L}{2\Lambda}+QE_0'\right)\sin 2\alpha=0, \tag{12}$$

which yields two angles $\alpha=0$ and $\pi/2$, i.e., the vertical or horizontal orientation of the rod is possible. Condition for the stable angle, which we get from the second derivative, is $\partial^2U_\Sigma/\partial\alpha^2\propto(\mathcal{K}-1)\cos 2\alpha>0$, where we introduced the ''orientation parameter'':

$$\mathcal{K}=\left(\frac{e|E_0|L}{\gamma_r T_e}\right)\frac{\ell_E}{L}\equiv\frac{2d\ell_E}{D}.$$

This shows that the quadrupole moment is important for the orientation—the equilibrium is determined by the competition between the dipole and quadrupole terms in energy (11). The dipole torque turns the rod along the electric field, whereas the quadrupole torque tends to make it horizontal. Hence, particles levitate horizontally, $\alpha=\pi/2$, when $\mathcal{K}<1$, and vertically, $\alpha=0$, when $\mathcal{K}>1$. Using the equilibrium condition in the vertical direction, $m_r g \simeq QE_0$, we eliminate the dependence on E_0 in the expression for $\mathcal{K}$, and applying the relation between γ_r and Q we derive the following scaling: $\mathcal{K}\propto\Lambda^2 a^4 E_0'^{-1}(\gamma_r T_e)^{-3}$. If we assume that γ_r does not depend on L and $E_0'=$const (the latter is usually true for rf sheaths), then $\mathcal{K}\propto\Lambda^2$. Therefore, the relative contribution of the dipole term is stronger for a longer rod: If Λ is sufficiently large the rod can levitate vertically, but for smaller Λ the horizontal orientation is more preferable.

Let us make an important remark concerning the equilibrium orientation. Figure 3 shows that the value of the particle charge, Q, might change considerably between vertical and horizontal orientations. This means that the charge is a certain function of the angle. Therefore, in general, the interaction with the electric field cannot be expressed in terms of the potential energy (similarly, for a particle with the space-dependent charge). In order to derive the equilibrium orientation, it is necessary to study the torque balance. We can present the charge versus angle dependence in the form $Q(\alpha)=Q_0[1+f(\alpha)]$, where $f(\alpha)$ is a certain even function of the angle. For the qualitative analysis, let us consider the following simple case: $f(\alpha)=\epsilon\sin^2\alpha$, where ϵ is a constant. The torque balance is given by Eq. (12) from which (using the condition $m_r g\simeq QE_0$) we obtain $\mathcal{K}_0-(1+\epsilon\sin^2\alpha)^3=0$, where $\mathcal{K}_0$ corresponds to Q_0. This equation has a solution for a certain angle, $0<\alpha_*<\pi/2$, if $\mathcal{K}_0$ is within the following range:

$$1<\mathcal{K}_0<(1+\epsilon)^3. \tag{13}$$

Simple analysis shows that this solution is always unstable, but instead *both* $\alpha=0$ and $\pi/2$ become stable. This means that two ''phases'' can coexist, consisting of identical rods levitating either vertically or horizontally, with the number fractions $2\alpha_*/\pi$ and $1-2\alpha_*/\pi$, respectively. When $\mathcal{K}_0$ is out of the (13), there is only one stable orientation—horizontal for $\mathcal{K}_0<1$ and vertical for $\mathcal{K}_0>(1+\epsilon)^3$, such as in the case of a constant charge.

VI. ROLE OF THE ION DRAG FORCE

In addition to the gravitational and electric forces, the ion drag force associated with momentum transfer from moving ions can influence the equilibrium states of the rods. Below we estimate the magnitude of the ion drag force acting on the horizontal and vertical rod. For monoenergetic ions the ion drag force is $F_{id}=n_i m_i u^2\sigma$, where $\sigma=\sigma^c+\sigma^s$ is the corresponding momentum transfer cross section [26,27]. It consists of the collection part (σ^c, due to the ion absorption) and the orbital part (σ^s, due to the elastic scattering in the field of the rod).

The absorption cross section is determined by the absorption radius, $\rho_{h,v}$. For a horizontal rod $\sigma_h^c=2\rho_h L$, whereas for a vertical rod, $\sigma_v^c=\pi\rho_v^2$. To estimate the scattering cross section, we consider two ranges of the impact parameter: ''Large'' $\rho\gtrsim\rho_*\sim L$ and ''moderate'' $\rho_{h,v}\lesssim\rho\lesssim\rho_*$. At large ρ, the electric potential is of the (screened) Coulomb form, and therefore the contribution of this range to the scattering cross section is roughly the same for both orientations, $\sim\pi L^2(\mathcal{E}_Q/\mathcal{E}_u)^2\ln(\lambda_{De}/\rho_*)$ [28]. [We remind that for our conditions ions are (super)sonic and, hence, do not contribute to the screening.] At moderate ρ one can use an approximate expression for potential (1) at $\rho\ll L$. We also assume that ions are deflected weakly. For a horizontal rod the deflection angle is $\simeq\pi(\mathcal{E}_Q/\mathcal{E}_u)$, which yields the following contribution to the scattering cross section: $\sim\pi^2L^2(\mathcal{E}_Q/\mathcal{E}_u)^2(\rho_*-\rho_h)/L$, whereas for a vertical rod (using the kinetic energy conservation) we get $\sim\pi L^2(\mathcal{E}_Q/\mathcal{E}_u)^2\ln(\rho_*/\rho_v)$. Thus we can finally estimate the scattering cross sections for the horizontal and vertical rods ($\rho_{h,v}\ll L\ll\lambda_{De}$),

$$\sigma_{h,v}^s\sim\pi L^2\left(\frac{\mathcal{E}_Q}{\mathcal{E}_u}\right)^2\times\begin{cases}[\pi+\ln(\lambda_{De}/L)] & \text{(horizontal)}\\ \ln(\lambda_{De}/\rho_v) & \text{(vertical)}.\end{cases}$$

Let us evaluate the role of the ion drag force for the conditions of experiments [12,13]. We choose the following plasma parameters: $n_i\sim n_e\sim 10^8$ cm^{-3}, $T_e\sim 1$ eV, and consider the rod with $L\sim 300$ μm and $L/a\sim 10^2$. For $M\gtrsim 1$, we obtain that the ion drag on a horizontal rod is mostly associated with the elastic ion scattering, while for a vertical rod the absorption dominates. Comparison of the ion drag force with gravity gives $F_{\rm id}/m_r g\lesssim 3\times 10^{-2}$ for both orientations. This allows us to conclude that for typical experimental conditions, the ion drag should not noticeably influence the rod equilibrium.

VII. INTERACTION OF CHARGED RODS

Rodlike particles levitating in rf sheaths or dc striations interact with each other and for certain conditions arrange themselves in ordered structures, as shown in Fig. 1. In order to reveal features of the interaction and understand difference from the case of spherical particles, one has to study the pair coupling energy of rods. Rods are polarized due to the presence of electric field, and the charge distribution along the rod axis is determined by Eq. (7). Using the formula $\phi_r(\mathbf{r})=\int_{-L/2}^{L/2}\lambda(z')|\mathbf{r}-\mathbf{z}'|^{-1}dz'$, we derive the following expression for the potential around the rod (in the cylindrical coordinates):

$$\phi_r(\rho,z)=\left(\lambda_0+\frac{E_0 z}{2\Lambda}\cos\alpha\right)[\ln(\xi_+ +\sqrt{\xi_+^2+1})+\ln(\xi_- +\sqrt{\xi_-^2+1})]+\frac{E_0\rho}{2\Lambda}\times\cos\alpha(\sqrt{\xi_-^2+1}-\sqrt{\xi_+^2+1}). \tag{14}$$

The deviations of Eq. (14) from the potential of a uniformly charged rod [Eq. (1)] are the polarization terms proportional

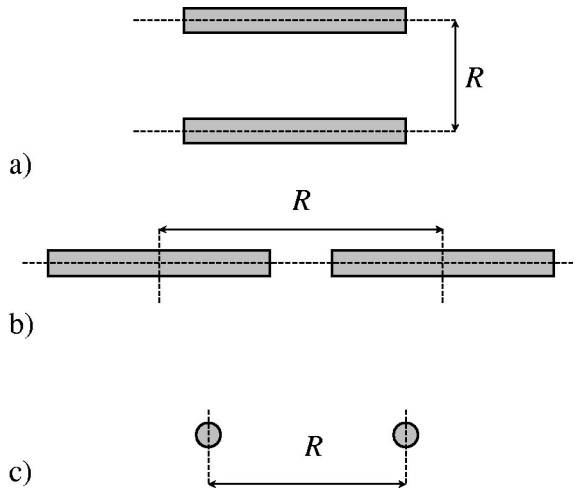

FIG. 6. Top view on three configurations of a pair of parallel rods: (a) Horizontal rods with parallel axes; (b) horizontal rods with common axis; (c) vertical rods with parallel axes.

to E_0. At large distances (but within the Debye sphere, $r \lesssim \lambda_{De}$), Eq. (14) has the following asymptotic multipole expansion (in spherical coordinates):

$$\phi_r(r,\theta) = \frac{Q}{r} + \frac{d}{r^2}\cos\alpha\cos\theta + \frac{D}{4r^3}(3\cos^2\theta - 1) + O(r^{-4}),$$

where $r=\sqrt{\rho^2+z^2}$ and $\cos\theta = z/r$. The dipole and quadrupole moments d and D are given by Eqs. (9) and (10), respectively.

Experiments [12,13] show that vertically and horizontally levitating particles never mix but separate into two ''phases,'' as shown in Fig. 1. Therefore, in order to study interaction within these phases it is sufficient to consider cases of horizontal or vertical particles separately. The pair coupling energy of two parallel rods with the centers separated by the distance (ρ,z) is

$$U_{rr}(\rho,z) = \int_{-L/2}^{L/2} \lambda(z')\phi_r(\rho, z+z')dz'. \qquad (15)$$

Now we can investigate major possible configurations relevant to experiments [12,13].

A. Horizontal rods with parallel axes

This case is shown in Fig. 6(a). Two horizontally levitating rods ($\alpha=\pi/2$) have parallel axes ($\rho>0$ and $z=0$ in cylindrical coordinates, or $\theta=\pi/2$ and $r=\rho$ in spherical coordinates); the dipole moment equals zero. Substituting potential (14) into expression (15), after simple integration we derive the coupling energy as a function of spherical coordinates:

$$U^h_{\rm rr}(r,\pi/2) = 2L\lambda_0^2\left[\operatorname{arcsinh}\frac{1}{\tilde r} - \sqrt{\tilde r^2+1} + \tilde r\right],$$

where $\tilde r = r/L$ is the dimensionless distance between the rods. The multipole expansion yields

$$U^h_{\rm rr}(r,\pi/2) = \frac{Q^2}{r} - \frac{QD}{2r^3} + O(r^{-4}). \qquad (16)$$

Using expression (10) for the quadrupole moment $D\propto Q$, we find that the relative correction of the charge-quadrupole term to energy (16) is $\simeq -\frac{1}{12}\tilde r^{-2}$. Hence, starting from $r \simeq L$ the charge-quadrupole and higher terms do not play an important role in pair interaction, and the coupling is actually determined by the charge-charge term only, such as in the case of spherical particles.

B. Horizontal rods with common axis

This case is shown in Fig. 6(b). Two horizontal rods have common axis ($\rho=0$ and $|z|>0$ in cylindrical coordinates, or $\theta=0$ and $r=|z|$ in spherical coordinates). Of course, we assume that r exceeds L. The coupling energy is

$$U^h_{\rm rr}(r,0) = L\lambda_0^2\left[2\tilde r\ln\frac{\sqrt{\tilde r^2-1}}{\tilde r} + \ln\frac{\tilde r+1}{\tilde r-1}\right],$$

with the multipole expansion

$$U^h_{\rm rr}(r,0) = \frac{Q^2}{r} + \frac{QD}{r^3} + O(r^{-4}). \qquad (17)$$

The relative correction of the charge-quadrupole term is $\simeq \frac{1}{6}\tilde r^{-2}$. Thus, it is sufficient to retain just the first charge-charge term at $r \gtrsim L$.

C. Vertical rods with parallel axes

This case is shown in Fig. 6(c). Vertically oriented ($\alpha=0$) rods are separated by $\rho>0$ and $z=0$ in the cylindrical coordinates, or $\theta=\pi/2$ and $r=\rho$ in spherical coordinates. The rods have the induced dipole moments, and the coupling energy is

$$U^v_{\rm rr}(r,\pi/2) = 2L\lambda_0^2\left[\operatorname{arcsinh}\frac{1}{\tilde r} - \sqrt{\tilde r^2+1} + \tilde r\right] + \frac{L}{24}\left(\frac{E_0L}{\Lambda}\right)^2\left[\operatorname{arcsinh}\frac{1}{\tilde r} + 3\tilde r - \frac{7}{3}\sqrt{\tilde r^2+1} - \frac{4}{3}\tilde r^2\sqrt{\tilde r^2+1} + \frac{4}{3}\tilde r^3\right].$$

Due to symmetry, the charge-dipole interaction terms cancel out, and the multipole expansion contains the charge-charge, dipole-dipole, and charge-quadrupole terms:

$$U^v_{\rm rr}(r,\pi/2) = \frac{Q^2}{r} + \frac{2d^2 - QD}{2r^3} + O(r^{-4}). \qquad (18)$$

Contribution of the dipole-dipole coupling is negligible, since $d^2/QD \equiv \frac{1}{24}(e|E_0|L/\gamma_r T_e)^2 \ll 1$, in accordance with the condition imposed for Eq. (7). The relative correction of the charge-quadrupole term, $\simeq -\frac{1}{12}\tilde{r}^{-2}$, is small at distances longer than the rod length.

The derived asymptotic expansions for the pair coupling energy, Eqs. (16)–(18), allow us to conclude that the interaction between the rods suspended in an external electric field is very similar to the interaction between the spherical particles. Despite of the fact that the potential of the rodlike particle can have considerable dipole and quadrupole terms, the *charge-charge coupling prevails* at distances about the rod length and higher.

VIII. DISCUSSION AND CONCLUSIONS

Experiments [12,13] performed with rodlike particles in rf and dc plasmas revealed a few general and interesting features common for both types of the discharge. First of all, it was rather difficult to find a proper range of discharge parameters where rods can be suspended—e.g., relatively high discharge power was necessary, as we mentioned in the Introduction. Simultaneous levitation of rods and spherical particles of similar diameter in a rf sheath demonstrated that spheres are always suspended higher than rods. This agrees with our theoretical results described in Sec. V, where we showed that the charge-to-mass ratio for rods is always smaller than that for spheres of the same radius. Hence, in order to levitate rods, much higher gradients of the electrostatic potential in sheaths or striations are necessary. The gradients increase with rf or dc discharge power—this is the reason why relatively high power is necessary in experiments.

Another interesting feature is that both in rf and dc discharges, the rods in horizontal planes arrange themselves in hexagonal structures. Also, in dc discharges it was possible to form multiple layer clouds, with an almost equidistant layer separation. Crystal structures formed by rods look very similar to those observed in experiments with spherical particles [1–5,29,30]. These observations support the results of Sec. VII, where we analyze electrostatic coupling between rods and show that it should be, in general, very similar to the interaction between spheres. This ''similarity in interaction'' can also relieve significantly the numerical simulation of plasma crystals formed by rodlike particles: In order to calculate the coupling energy, it is quite sufficient to use just first three terms in the multipole expansion of the rod potential, i.e., treat rods as pointlike particles with given charge, dipole, and quadrupole moments.

The major difference found between the experimental results [12,13] for rf and dc discharges is the following: In dc plasma, all rods (''short,'' of $L \simeq 300$ μm, and ''long,'' of $L \gtrsim 600$ μm) were always oriented horizontally, but in rf plasma short particles were suspended vertically, whereas long particles levitated horizontally. Also, the latter seems to be in contradiction with theoretical conclusions made in Sec. V—short rods should levitate horizontally, but for sufficiently long particles the vertical orientation is more preferable. However, the theoretical analysis of equilibrium states in Secs. IV and V requires the external electric field (which provide the levitation) to be weakly inhomogeneous—the spatial scale of the field variation ℓ_E should be larger than the rod length L. The field inhomogeneity is estimated as $\ell_E \simeq 0.6$ mm for experiments in rf sheaths [13,31], and is believed to be a few times larger for experiments in dc striations [5,12]. Hence, we can use the weakly inhomogeneous field approximation for the analysis of experiments in dc plasmas, where the condition $\ell_E \gtrsim L$ is satisfied both for short and long rods. This approximation is also applicable for short particles in rf sheaths. For long rods in a rf discharge, however, one has to take into account the strong field inhomogeneity.

Let us apply the results of Sec. V for the analysis of particle orientation observed in the experiments. It is convenient to rewrite the orientation parameter in the form $\mathcal{K} = (2\Lambda e^2 m_r g/L)(\ell_E/\gamma_r^2 T_e^2)$. The first factor characterizes size and mass of a rod, while the second one is a function of local plasma parameters. The orientation of identical particles in different plasma conditions is thus determined by the value of the second factor, i.e., by three parameters: ℓ_E, γ_r, and T_e. For short particles in rf sheath we estimate $\mathcal{K} \simeq 1.5$, assuming $\gamma_r \simeq 3.5$ (high-M limit) and $T_e \sim 1$ eV. Therefore, $\mathcal{K}$ can exceed unity and the short rods should orient themselves vertically, in accordance with the experimental observations. In dc striations, where all gradients are much weaker compared to those in rf sheaths, one can expect much smaller Mach numbers and thus—higher values of γ_r (see Fig. 3). In addition, the electron temperature is believed to be much higher in striations [5,12] (in the head of a striation, the electron energy spectrum is dominated by the energies close to the first excitation level, which is $\simeq 16.6$ eV for neon). Contribution of higher T_e and γ_r to the expression for $\mathcal{K}$ can easily overcome the increase due to higher ℓ_E and thus make the resulting value of the orientational parameter smaller. Therefore, in dc striations $\mathcal{K}$ can be less than unity and then the short rods levitate horizontally. The orientational parameter is increased logarithmically for long rods [by $\simeq (15–20)\%$], but this relatively small variation might not be sufficient to set the orientation parameter above the threshold unity. Presumably, this is why long rods also levitate horizontally in dc striations. Thus, one can see that the proposed theory for the orientation (Sec. V), when applicable, is in qualitative agreement with experiments.

For long particles in rf sheaths, i.e., when the field is strongly inhomogeneous ($\ell_E < L$), the balance of torques which determines the rod orientation is quite different from that derived in Sec. V. Let us consider the vertically oriented rod in the limit $\ell_E \ll L$. In this case, a significant electric field exists only in the vicinity of the lower tip of the rod. Therefore, the torque due to the dipole moment should be relatively small (compared to the weakly inhomogeneous case). In contrast, the quadrupole moment torque should be increased, since the center of the electric force will be shifted from the center downward to the lower tip. Thus, the vertical orientation is obviously unstable in the strongly inhomogeneous case, and the only possible orientation is the horizontal one. Note that sometimes very long freak particles (of 1–3 mm length) were observed in a rf sheath floating hori-

zontally. This agrees with our theoretical conclusions made in Sec. V: The charge-to-mass ratio for horizontal particles has very weak logarithmic dependence on the length, and thus rods of quite broad length spectrum might be levitated.

One can think about new ''dedicated'' experiments which would allow us to test the model more carefully. First of all, using rods of various lengths and/or diameters, one can obtain an equilibrium orientation angle as a function of particle sizes, and compare this with the theoretical predictions. Particularly interesting issue to check is the possible coexistence of two ''phases'' consisting of identical rods, levitating either vertically or horizontally. Such an experiment would also allow us to verify another important prediction—rather strong dependence of the charge on the orientation (see Fig. 3): Observing difference in the levitation height of horizontal and vertical rods, one can easily estimate the charge difference. Another important experiment might be to compare the behavior of dielectric and conductive (coated) rods of the same size. (So far, there has been only one experiment with rods coated with a thin conductive layer [32]. It did not reveal, however, any difference in the behavior of the coated and noncoated particles.) Experiments where the mixture of rods of different sizes or rods and spherical particles are used can help us to explore possible phase states of complex plasmas with strongly asymmetric particles. Also, investigation of waves and instabilities in such systems would help us to test recently published theories [33,34].

The model proposed in this paper is an attempt of consistent theoretical analysis of complex plasmas with strongly asymmetric (rodlike) particles. Obviously, this model cannot provide universal description of the problem—there are various important physical processes which are not taken into account. For example, we limited the consideration by the case of conductive particles. The analysis of charging of dielectric particles oriented along the electric field (ion flux), being quite a difficult problem, might nevertheless be very important for interpretation of experiments. Also, we derived only asymptotic expressions for an equilibrium charge of vertical rods, in the limits of low and high ion Mach numbers. Of course, the range of moderate Mach numbers, $M \sim 1$, needs to be studied more rigorously. Taking into account ion-neutral collisions and plasma screening can be important, when considering relatively long particles (about 0.5 mm and longer) and/or high pressures (about 50 Pa and higher): In this case, all the characteristic lengths—particle length, ion mean free path, and the screening (Debye) length—become of the same order of magnitude. And finally, charging and equilibrium states of rods in strongly inhomogeneous electric fields need to be investigated.

ACKNOWLEDGMENT

A.G.K. gratefully acknowledges support from the Max Planck Society. A.V.I. was supported by DLR under Contract No. 50 WP 0203.

APPENDIX: ION FLUX ON VERTICAL ROD; FINITE ION TEMPERATURES

Consider the rod oriented along the flux of ions having a finite temperature T_i. The thermal velocity dispersion in the azimuthal direction implies nonzero angular momentum, which results in the appearance of a term $\propto \rho^{-2}$ in the effective potential energy for the radial ion motion [21]. This can significantly change trajectories of ions as they approach closer to the rod. Hence, we have to include into consideration the thermal angular momentum. Then, instead of Eq. (4) the resulting equation for the radial motion (averaged over the thermal distribution) is

$$\ddot{\tilde{\rho}} = -\frac{\mathcal{E}_Q}{\mathcal{E}_u}\frac{1}{\tilde{\rho}} + \frac{T_i}{\mathcal{E}_u}\frac{\tilde{\rho}_v^2}{\tilde{\rho}^3}. \tag{A1}$$

If the radial motion at the initial moment $\tau = 0$ is neglected $[\dot{\tilde{\rho}}(0) = 0]$, then integrating Eq. (A1) we get the following for the energy conservation:

$$\dot{\tilde{\rho}}^2 = 2\frac{\mathcal{E}_Q}{\mathcal{E}_u}\ln\frac{\tilde{\rho}_v}{\tilde{\rho}} - \frac{T_i}{\mathcal{E}_u}\left(\frac{\tilde{\rho}_v^2}{\tilde{\rho}^2} - 1\right). \tag{A2}$$

Equation (A2) demonstrates that the absorption radius for the vertical rod cannot exceed a limiting value, $\rho_v^{\lim}$, determined by the condition $\dot{\rho} = 0$ at $\rho = a$, which yields the equation $(\rho_v^{\lim}/a)^2 = 1 + 2(\mathcal{E}_Q/T_i)\ln(\rho_v^{\lim}/a)$. This limitation appears because at small ρ the angular momentum term changes faster than the electrostatic potential energy, and ions cannot approach the central axis infinitely close. Assuming $\mathcal{E}_Q/T_i \gg 1$, we can roughly estimate the upper limit for the absorption radius as $\rho_v^{\lim}/a \sim \sqrt{(\mathcal{E}_Q/T_i)\ln(\mathcal{E}_Q/T_i)}$.

In order to derive the absorption radius, one has to integrate Eq. (A2) with the absorption condition $\tilde{\rho}(1) = a/L$. Solution of Eq. (A2) depends on two parameters (or their combinations): $\beta = (L/a)^2(T_i/\mathcal{E}_u)$ and $\mathcal{E}_Q/T_i$. It turns out that the absorption condition can only be satisfied when β is sufficiently small and we are below the curve shown in Fig.

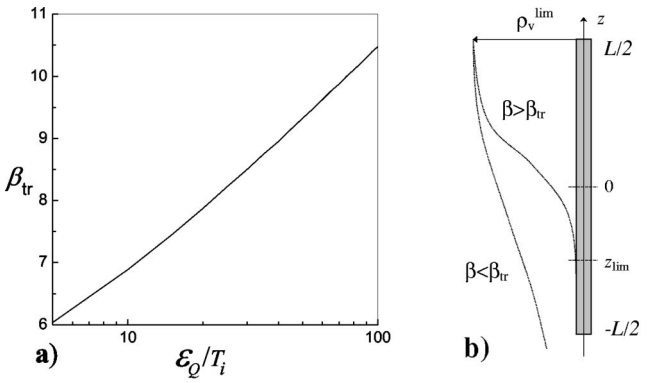

FIG. 7. (a) Transition value of parameter $\beta = (L/a)^2(T_i/\mathcal{E}_u)$ versus the ratio $\mathcal{E}_Q/T_i$, where L and a are the length and radius of the rod, and $\mathcal{E}_Q = e|Q|/L$ and $\mathcal{E}_u = \frac{1}{2}m_i u^2$ are the Coulomb and ion kinetic energies. For $\beta \geqslant \beta_{tr}$ the ion absorption is strongly affected by the thermal motion, for $\beta \ll \beta_{tr}$ the thermal motion is negligible. The curve $\beta = \beta_{tr}$ shows the transition between two regimes. (b) Ion trajectories for these regimes: If the thermal radial motion is not taken into account for $\beta > \beta_{tr}$, then all ions are absorbed at $z_{lim} \leqslant z \leqslant L/2$.

7(a): The absorption radius equals $\rho_v^{\lim}$ at the curve $\beta=\beta_{tr}$, and decreases monotonically as β decreases. At $\beta\to 0$ the absorption radius tends to the asymptote determined by Eq. (5). Low β implies high Mach numbers, since $\beta\equiv 2M^{-2}(L/a)^2(T_i/T_e)$. Therefore, in the high-M limit the absorption radius can be approximated by Eq. (5), and the particle potential (charge) is determined by the solution of Eq. (6) shown in Fig. 3 (dashed line). The range of Mach numbers for this limit can be evaluated from the condition $\beta\lesssim\beta_{\rm tr}$. From Fig. 7(a) we have $\beta_{\rm tr}\simeq 8$–9 [for the range $\mathcal{E}_Q/T_i\equiv\gamma_r(T_e/T_i)/2\Lambda\sim 20$–$40$, assuming $T_e/T_i\sim 10^2$ and $\gamma_r\sim 3$], and thus, the high-M limit is valid for $M\gtrsim\sqrt{2(T_i/T_e)/\beta_{\rm tr}}(L/a)\sim 3$.

For smaller M, when the parameter β is high enough ($\beta>\beta_{\rm tr}$) the absorption condition $\tilde{\rho}(1)=a/L$ for Eq. (A2) cannot be satisfied. In accordance with the solution, all ions with $\rho\leqslant\rho_v^{\lim}$ are absorbed in the range $z_{\lim}\leqslant z\leqslant L/2$, where $z_{\lim}>-L/2$ is the lowest absorption coordinate, as shown in Fig. 7(b). Therefore, if $\beta>\beta_{\rm tr}$, the concept that the initial radial velocity of the absorbed ions is equal to zero fails: Some ions can have infinitely large ρ at $z\to+\infty$, but due to the *thermal* motion towards the center they approach the rod sufficiently close and can be absorbed. This can be understood from the simple scaling: The radial thermal motion is important when the time which is needed for thermal ions to be absorbed (which is, using OML approximation, of the order of a few $a\sqrt{\gamma_r T_e/T_i}/\sqrt{\Lambda\mathcal{E}_Q/m_i}\sim a/v_{T_i}$) becomes comparable with the time during which ions pass the rod ($\simeq L/u$). From that we get the condition $(L/a)^2(T_i/\mathcal{E}_u)\equiv\beta\simeq$const, which is essentially the boundary shown in Fig. 7(a). [Note that the dependence $\beta_{\rm tr}$ versus $\mathcal{E}_Q/T_i$ is very weak (almost logarithmic), and since the variation of $\mathcal{E}_Q/T_i\propto\gamma_r$ is limited by a factor of a few (see Fig. 3), the boundary can be approximated by $\beta\simeq$const.] Thus, we can interpret the curve in Fig. 7(a) as a transition boundary between the two regimes, when the ion thermal motion affects the absorption strongly ($\beta\gtrsim\beta_{\rm tr}$), or weakly ($\beta\ll\beta_{\rm tr}$). For $\beta\gtrsim\beta_{\rm tr}$ the ion absorption at the lower part of the rod, at $-L/2\leqslant z\leqslant z_{\lim}$, is due to the thermal radial motion. As β increases further (M decreases), $z_{\lim}$ approaches $z=L/2$ and the fraction of the "thermal" ions in the total flux grows. Eventually, we end up with the case of an isotropic plasma, when the total ion flux on the rod is given by the OML expression for a cylindrical particle [19] ($J_i\simeq 2\rho_T L n_i v_{T_i}$ with $\rho_T\simeq a\sqrt{2\gamma_r T_e/T_i}$). Hence, at small M the particle potential is given by the low-M asymptote for a horizontal rod shown in Fig. 3 (solid line).

[1] J.H. Chu and L. I, Phys. Rev. Lett. **72**, 4009 (1994).
[2] H.M. Thomas *et al.*, Phys. Rev. Lett. **73**, 652 (1994).
[3] Y. Hayashi, and K. Tachibana, Jpn. J. Appl. Phys., Part 2 **33**, L804 (1994).
[4] V.E. Fortov *et al.*, JETP Lett. **64**, 92 (1996).
[5] A.M. Lipaev *et al.*, JETP **85**, 1110 (1997).
[6] N. Sato, G. Uchida, R. Ozaki, and S. Iizuka, in *Physics of Dusty Plasmas*, edited by Mihály Horany, Scott Robertson, and Bob Walch, AIP Conf. Proc. No. 446 (AIP, Woodbury, NY, 1998), p. 239.
[7] G.E. Morfill, H.M. Thomas, U. Konopka, and M. Zuzic, Phys. Plasmas **6**, 1769 (1999).
[8] A.P. Nefedov, O.F. Petrov, V.I. Molotkov, and V.E. Fortov, JETP Lett. **72**, 218 (2001).
[9] G.E. Morfill *et al.*, Plasma Phys. Controlled Fusion **44**, B263 (2002).
[10] H. Löwen, J. Chem. Phys. **100**, 6738 (1994).
[11] H. Graf, *Freezing Transitions in Liquid Crystals* (Shaker, Aachen, 1998).
[12] V.I. Molotkov *et al.*, JETP Lett. **71**, 102 (2000).
[13] B.M. Annaratone *et al.*, Phys. Rev. E **63**, 036406 (2001).
[14] U. Mohideen *et al.*, Phys. Rev. Lett. **81**, 349 (1998).
[15] P.J. Hagris *et al.*, Rev. Sci. Instrum. **65**, 140 (1994).
[16] L.D. Landau and E.M. Lifshitz, *Electrodynamics of Continuous Media* (Pergamon, Oxford, 1960).
[17] J.D. Jackson, *Classical Electrodynamics* (Wiley, New York, 1963).
[18] V.N. Tsytovich, Phys. Usp. **40**, 53 (1997).
[19] J.E. Allen, Phys. Scr. **45**, 497 (1992).
[20] E.G. Whipple, Rep. Prog. Phys. **44**, 1197 (1981).
[21] P.M. Chung, L. Talbot, and K.J. Touryan, *Electric Probes in Stationary and Flowing Plasmas: Theory and Application* (Springer, New York, 1975).
[22] Yu.P. Raizer, *Gas Discharge Physics* (Springer, Berlin, 1991)
[23] S.D. Hester and A.A. Sonin, Phys. Fluids **13**, 1265 (1970).
[24] G.E. Morfill *et al.*, Phys. Rev. Lett. **83**, 1598 (1999).
[25] L.D. Landau and E.M. Lifshitz, *The Classical Theory of Fields* (Pergamon, Oxford, 1962).
[26] M.S. Barnes *et al.*, Phys. Rev. Lett. **68**, 313 (1992).
[27] S.A. Khrapak, A.V. Ivlev, G.E. Morfill, and H.M. Thomas, Phys. Rev. E **66**, 046414 (2002).
[28] L.D. Landau and E.M. Lifshitz, *Physical Kinetics* (Pergamon, Oxford, 1981).
[29] Y. Hayashi, Phys. Rev. Lett. **83**, 4764 (1999).
[30] M. Zuzic *et al.*, Phys. Rev. Lett. **85**, 4064 (2000).
[31] U. Konopka, Ph.D. thesis, München, 2000.
[32] V.E. Fortov *et al.*, in *Proceedings of the International Conference on Phenomena in Ionized Gases, Nagoya, 2001*, edited by T. Goto (Nagoya University, Nagoya, 2001), Vol. 3, p. 35.
[33] S.V. Vladimirov and E.N. Tsoy, Phys. Rev. E **64**, 035402(R) (2001).
[34] J. Mahmoodi, P.K. Shukla, N.L. Tsintsadze, and D.D. Tskhakaya, Phys. Rev. Lett. **84**, 2626 (2000).